Bull Earthquake Eng (2009) 7:547–573
DOI 10.1007/s10518-009-9111-z

ORIGINAL RESEARCH PAPER

Seismic response of single-column bent on pile: evidence of beneficial role of pile and soil inelasticity

Nikos Gerolymos · V. Drosos · G. Gazetas

Received: 26 November 2008 / Accepted: 17 March 2009 / Published online: 2 April 2009

Abstract While seismic codes do not allow plastic deformation of piles, the Kobe earthquake has shown that limited structural yielding and cracking of piles may not be always detrimental. As a first attempt to investigate the consequences of pile yielding in the response of a pile-column supported bridge structure, this paper explores the soil–pile-bridge pier interaction to seismic loading, with emphasis on structural nonlinearity. The pile–soil interaction is modeled through distributed nonlinear Winkler-type springs and dashpots. Numerical analysis is performed with a constitutive model (Gerolymos and Gazetas 2005a, Soils Found 45(3):147–159, Gerolymos and Gazetas 2005b, Soils Found 45(4):119–132, Gerolymos and Gazetas 2006a, Soil Dyn Earthq Eng 26(5):363–376) materialized in the OpenSees finite element code (Mazzoni et al. 2005, OpenSees command language manual, p 375) which can simulate: the nonlinear behaviour of both pile and soil; the possible separation and gapping between pile and soil; radiation damping; loss of stiffness and strength in pile and soil. The model is applied to the analysis of pile-column supported bridge structures, focusing on the influence of soil compliance, intensity of seismic excitation, pile diameter, above-ground height of the pile, and above or below ground development of plastic hinge, on key performance measures of the pier as is: the displacement (global) and curvature (local) ductility demands and the maximum drift ratio. It is shown that kinematic expressions for performance measure parameters may lead to erroneous results when soil-structure interaction is considered.

Keywords Dynamic soil-structure interaction · Soil and pile inelasticity · Seismic performance measures · Extended pile shaft-supported bridge

N. Gerolymos (✉) · V. Drosos · G. Gazetas
National Technical University, Athens, Greece
e-mail: gerolymos@gmail.com

1 Introduction

Current seismic design of bridge structures is based on a presumed ductile response. A capacity design methodology ensures that regions of inelastic deformation are carefully detailed to provide adequate structural ductility, without transforming the structure into a mechanism. Brittle failure modes are suppressed by providing a higher level of strength compared to the corresponding to ductile failure modes. For most bridges, the foundation system may be strategically designed to remain structurally elastic while the pier is detailed for inelastic deformation and energy dissipation. Essentially-elastic response of the foundation is usually ensured by increasing the strength of the foundation above that of the bridge pier base so that plastic hinging occurs in the pier instead of the foundation.

The concept of ductility design for foundation elements is still new in earthquake engineering practice. The potential development of a plastic hinge in the pile is forbidden in existing regulations, codes and specifications. The main reasons are: (i) the location of plastic hinges is not approachable for post-seismic inspection and repair, (ii) the high cost associated with repair of a severely damaged foundation, and (iii) failure due to yielding in the pile prior to exceeding soil capacity is an undesirable failure mechanism, by contrast to that in which soil capacity is mobilized first.

However, several case-histories (especially from the Kobe 1995 earthquake) have shown that: (a) pile yielding under strong shaking cannot be avoided, especially for piles embedded in soft soils; and (b) pile integrity checking after an earthquake is a cumbersome, yet feasible task. Furthermore, there are structures where plastic hinging cannot be avoided in members of the foundation during a severe earthquake. A good example of such structure is the *pile-column* (also known in the American practice as *extended pile-shaft*), where the column is continued below the ground level as a pile of the same or somewhat larger diameter. Obviously, the design of such foundation requires careful consideration of the flexural strength and ductility capacity of the pile.

An advantage of supporting a column bent on drilled pile is the cost savings associated with the construction of large cast-in-drilled-hole (CIDH) piles instead of multiple piles of smaller diameter, which must later be integrated into a structural unit using a pile cap. Another advantage of such a design is that localized damage that could otherwise develop at the column-pile cap joint is avoided by the pile-column combination, since there is no structural distinction between the pile and the column other than the presence of a construction joint at the pile-column interface.

While the design of piled footings favors forcing plastic "hinging" into the superstructure, with the piles remaining elastic, pile-columns can be designed with overall ductile performance in mind. In case of a single pile-column, formation of a plastic hinge in the pile shaft is the only mechanism by which ductile performance can be attained. A pile-column bent may first tend to plastify at the column-beam joint, but the full flexural capacity of the system can only be obtained through the formation of a secondary plastic hinge, below ground surface (at least slightly below). Bending moment distribution varies with height, but diminishes after attaining a maximum bending moment below the ground level. A typical depth for maximum bending moment, and possibly the location of the plastic hinge, ranges from one to three or four pile diameters below ground surface, depending on the above-ground height and soil stiffness.

Damage below ground in the form of cracking or spalling of concrete, fracture of transverse reinforcement, or buckling of longitudinal reinforcement is generally difficult to assess after an earthquake. This, coupled with the potential high cost of repair, resulted in the current use of a design displacement ductility factor that is smaller than that of columns in order to

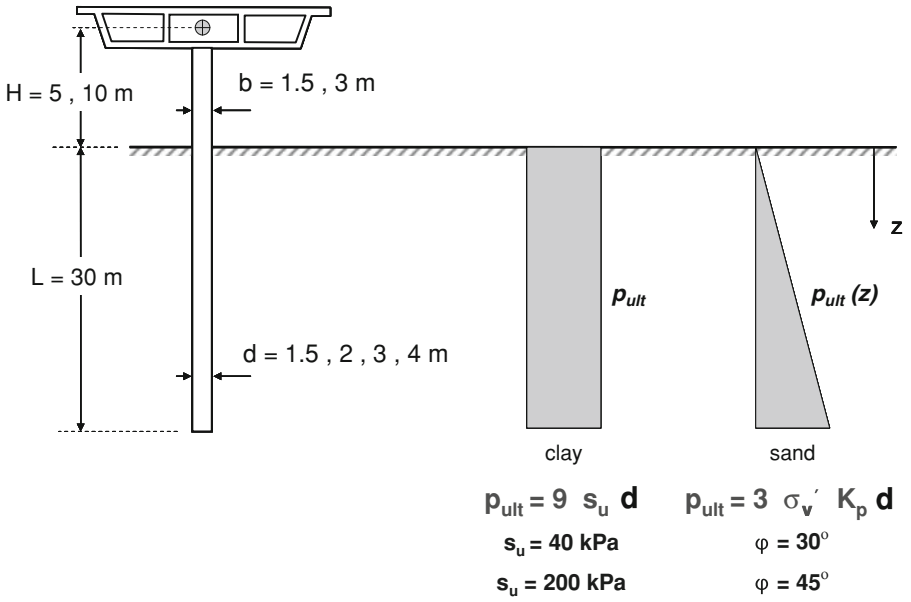

Fig. 1 The problem investigated and the two types of presumed soil deposits

limit the amount of yielding in the pile below the ground level. For example, in the United States, ATC-32 (ATC 1996) prescribes a displacement ductility factor of 3 for pile-columns compared to a displacement ductility factor of 4 for well-confined fixed-base reinforced concrete columns. A similar approach of prescribing higher lateral strength for piles has been adopted for seismic design of highway bridges in New Zealand. For plastic hinging that may develop at a depth less than 2 m below the ground level, but not below the mean water level, the design displacement ductility factor is limited to no more than 4. For plastic hinging at a depth greater than 2 m below the ground level or below the mean water level, the design displacement ductility factor is reduced to no more than 3 (Chapman 1995; Park 1998).

In this paper, a parametric investigation of the nonlinear inelastic response of pile-column bridge systems is conducted, and the influence of pile inelastic behavior and soil-structure interaction on structure ductility demand is identified. The role of various key parameters are examined, such as: (a) soil compliance, (b) above-ground height of the column shaft, (c) pile diameter, (d) intensity of the input seismic motion, and (e) location of the plastic hinge, on characteristic performance measures of the soil-structure system response, such as: the displacement (global), $\mu_{\delta,}$ and curvature (local), $\mu_{\varphi,}$ ductility demands and the maximum drift ratio γ_{max}. It is shown that: (a) neglecting the consideration of the soil-structure interaction effects may lead to unconservative estimates of the actual seismic demand, and (b) the development of a plastic hinge along the pile (for instance for cases that the pile is designed with inferior or equal strength compared to that of the pier) is beneficial for the pier response.

2 The problem: equations and parameters

2.1 Definition of the problem

The studied problem is sketched in Fig. 1: a pile-column embedded in clay or sand deposit, monolithically connected to the bridge deck is excited by a seismic motion. It is assumed

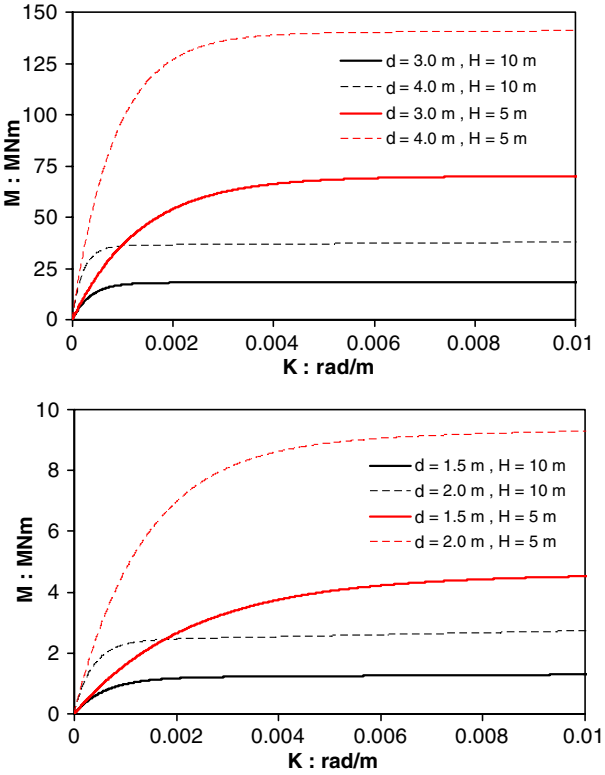

Fig. 2 Predefined moment–curvature relations used in the analyses

that the transverse response of the bridge structure may be characterized by the response of a single bent, as would be the case for a regular bridge with coherent ground shaking applied to all bents.

The height of the pier H is given parametrically the values of 5 and 10 m, so that a typical urban bridge and a rather short viaduct, in respect, are examined. The diameter b of the pile-column above-ground takes values of 1.5 and 3.0 m. However, to investigate the influence of the plastic hinge position on the system response, two more cases are examined: the below-ground pile-column diameter d is increased by 33% relatively to the above-ground diameter b. So, for pile diameters $b = 1.5$, 2.0, 3.0, and 4.0 m, pier diameter equals to $b = 1.5$, 1.5, 3.0, and 3.0 m, respectively. For sake of simplicity, the term *diameter* will refer from this point on, to the below-ground diameter d. The embedment length of the pile L is considered in every case equal to 30 m. In total, a set of four structural configurations are analysed.

The mass of the deck is calculated so that the fundamental period of the fixed-base pier would be $T = 0.3$ sec for all cases studied. This restriction for the fixed-base period leads to a mass of 45 mg for the pile diameter of $d = 1.5$ m, and 720 mg for that of $d = 3.0$ m. The nonlinear behavior of the pile-column is characterized through the predefined moment–curvature relations illustrated in Fig. 2. These curves have been obtained with the BWGG model (Gerolymos and Gazetas 2005b), discussed in the sequel, for $n = 1$, initial stiffness equal to the uncracked flexural stiffness EI of the pile-column, and ultimate strength equal to the conventionally calculated moment at the ground surface considering that a critical

acceleration of 0.2 g is applied on the deck mass. In the case of the variable-diameter piers, the bending moment capacity of the pile cross-sections is calculated to be proportional to the square power of the cross-section diameter d^2, which is a reasonable assumption for a given detailing of reinforcement. In that way, the potential development of a plastic is forced to occur in the above-ground portion of the pile-column.

It is noted that the objective of the parametric study described herein is to investigate the seismic response of the system in the inelastic regime and not to design the structure. Therefore, (a) we are mainly concerned about achieving equivalence of the studied systems in the framework of nonlinear response analysis without considering soil-structure interaction effects, rather than about reinforcement details that correspond to the utilized moment–curvature curves. And (b) the critical acceleration was scaled to 0.2 g, to ensure that the system will enter the inelastic regime under the used seismic excitation.

2.2 Constitutive equations and numerical modeling

The developed BWGG model is a versatile one-dimensional action–reaction relationship, capable of reproducing an almost endless variety of stress–strain or force–displacement or moment–rotation relations, monotonic as well as cyclic. It is being applied here to model the monotonic and cyclic response of piles, expressing both the p–y and moment–curvature relationships. A simple version of the model is outlined below. More details can be found in Gerolymos and Gazetas (2005a,b, 2006a,b), although the model utilized here is a slightly improved-simplified version of the model in the latter reference.

The lateral soil reaction against a deflecting pile is expressed as the sum of an elastic, and an inelastic component according to:

$$p_x = \alpha_s k_s y + (1-\alpha_s) p_y \zeta_s \tag{1}$$

where ζ_s is a dimensionless inelastic soil parameter expressed in the following differential form:

$$\frac{d\zeta_s}{dy} = \frac{\eta_s h_s}{y_0}\left\{1 - |\zeta_s|^{n_x}\left[b_s + g_s sign(dy\zeta_s)\right]\right\} \tag{2}$$

where p_x is the resultant (in the direction of loading) of the normal and shear stresses along the perimeter of a pile segment of unit length and it includes both "in-phase" and "out-of-phase" components; the latter reflects radiation and hysteretic damping in the soil. y is the pile deflection at the location of the spring; k_s is a reference spring stiffness; α_s is a parameter governing the post yielding stiffness; p_y is a characteristic value of the soil reaction related to the initiation of significant inelasticity (yielding); y_0 is a characteristic value of pile deflection related to the initiation of yielding in soil reaction. n_s, b_s and g_s, are dimensionless quantities that control the shape of the hysteretic soil reaction-pile deflection loop, and η_s, r_s and h_s are strain hardening parameters for stiffness decay, strength degradation, and pinching behaviour, respectively; where c_s is the damping coefficient at small amplitude motions, and c_{sd} is a viscoplastic parameter which controls the coupling of soil and soil–pile interface nonlinearity with radiation damping. The reader is referred to Gerolymos and Gazetas (2005a,b) for more details.

The inelastic behaviour of the pile is similarly expressed in terms of a strength-of-materials-type bending moment–pile curvature relation, which includes an elastic and an inelastic component:

$$M = \alpha_p E_p I_p \frac{\partial^2 y}{\partial z^2} + (1-a_p) M_y \zeta_p \tag{3}$$

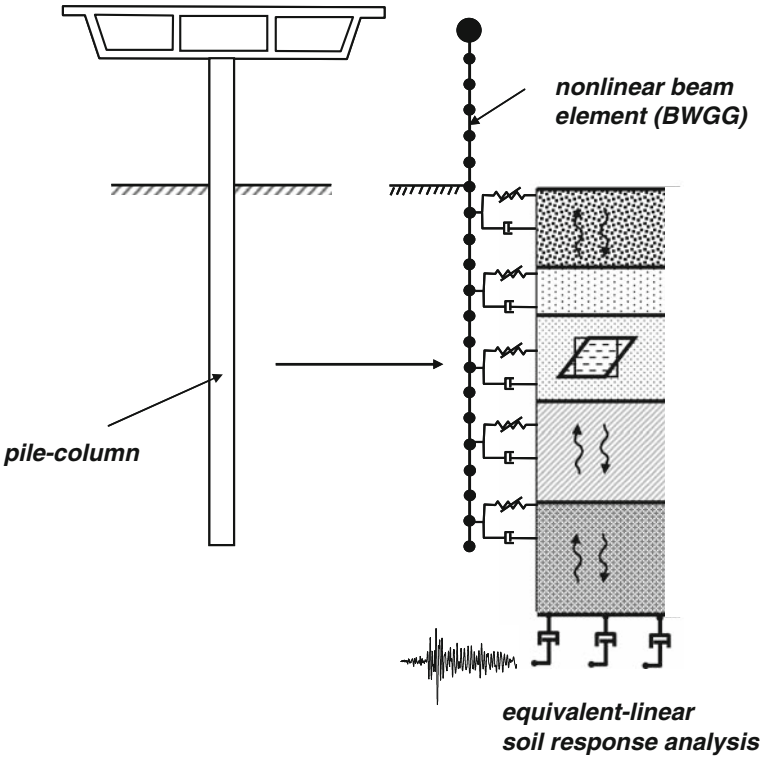

Fig. 3 Schematic illustration of the model used for the analyses

where $E_p I_p$ is the initial (elastic) bending stiffness (also called flexural rigidity), α_p is a parameter controlling the post yielding bending stiffness, M_y is the value of bending moment that initiates structural yielding in the pile, and ζ_p is the hysteretic dimensionless parameter which controls the nonlinear structural response of the pile. The latter is governed by

$$\frac{d\zeta_p}{d\kappa} = \frac{\eta_p h_p}{\kappa_0}\left\{1 - \left|\zeta_p\right|^{n_p}\left[b_p + g_p sign(d\kappa\zeta_p)\right]\right\} \tag{4}$$

where κ is the pile curvature, and $b_p, g_p, n_p, \eta_p, r_p$, and h_p,are dimensionless quantities that control the shape of the hysteretic bending moment–curvature loop in the same manner as $n_s, b_s, g_s, \eta_p, r_p$, and h_p, control the shape of the lateral soil reaction–deflection loop. κ_0 is the value of pile curvature at *initiation of yielding* in the pile.

Evidently, Eqs. 3–4 are of the same form as Eqs. 1–2, except that no viscous term (radiation damping) is included in the structural pile response.

The seismic response of the soil–pile-structure system is investigated herein via a beam-on-nonlinear-Winkler-foundation (BNWF) finite element model developed in OpenSees (Fig. 3).

The pile-column is discretized into nonlinear beam elements with length 0.5–1.0 m, whose bending behavior is governed by the macroscopic constitutive BWGG model. The mass of the deck is simulated as a concentrated mass at the top node of the pile-column, whereas the distributed mass of the extended pile is simulated by lumped masses on beam-element nodes.

The near-field soil-pile interface is simulated with nonlinear p–y spring elements, the behavior of which is described also by the BWGG model. Model parameters were appropriately calibrated to match the p–y curves of Reese et al. (1974) and Matlock (1970). The free extremities of the soil springs were excited by the acceleration time histories obtained at each depth from the free-field seismic response analysis (Banerjee et al. 1987).

Although the developed finite element model has the capability to reproduce higher order phenomena (e.g. P–Δ effects), such phenomena were ignored, considering that their strong dependence on the mass of the structure and the geometry would obscure the role of other parameters (e.g. structural inelasticity and soil compliance).

2.3 Soil parameters

The influence of near-field soil compliance on the seismic response of the soil–pile-structure system is investigated parametrically considering four different homogeneous soil profiles (Fig. 1): (a) sand with friction angle $\varphi = 30°$, (b) sand with friction angle $\varphi = 40°$, (c) clay with undrained shear strength $S_u = 40\,\text{kPa}$, and (d) clay with undrained shear strength $S_u = 200\,\text{kPa}$.

The small-amplitude stiffness $k(= p_y/y_0)$ was obtained from the available beam-son-dynamic-Winkler-Foundation solutions (e.g., Gazetas and Dobry 1984; Makris and Gazetas 1992) in terms of the Young's modulus of the soil.

For piles in cohesive soils the ultimate soil reaction per unit length of pile can be approximated by the well known expression

$$P_y = \lambda_1 S_u d \tag{5}$$

where S_u is the soil undrained shear strength, and λ_1 varies from 9 to 12, depending on the friction ratio f_s/S_u at the pile–soil interface. A value of $\lambda_1 = 9$ is often used for a soft clay, while $\lambda_1 = 11$ is more appropriate for a stiff clay. At shallow depths, the plane strain assumption of Eq. 8 is inappropriate because of the non-zero vertical deformation of the soil during lateral motion of the pile. The following formulation has been proposed for P_y near the surface (Matlock 1970)

$$P_y = \left(\lambda_2 + \frac{\sigma'_v}{S_u} + J\frac{z}{d}\right) S_u d, \quad z < \frac{(\lambda_1 - \lambda_2)d}{\frac{\gamma'_s d}{S_u} + J} \tag{6}$$

where σ'_v is the vertical effective stress, and γ'_s the effective specific weight of the soil, and λ_2 and J are a dimensionless quantities. Broms (1964a,b) proposed a value of $\lambda_2 = 2$, whereas Matlock (1970) used $\lambda_2 = 3$. Matlock (1970) stated that the value of J was determined experimentally to be 0.5 for a soft clay and about 0.25 for a medium clay, whereas Reese (1975) suggested a value of $J = 2.83$ for every type of clay. For piles embedded in cohesionless soils, Broms (1964a,b) proposed an analytical expression for the ultimate soil reaction:

$$P_y = 3\gamma'_s d \tan^2\left(45° + \frac{\varphi}{2}\right) z \tag{7}$$

where φ is the angle of friction. Equation (7) is very often preferred in practice among other more rigorous expressions for its simplicity and compatibility with experimental results.

For the description of the nonlinear behavior of the near-field soil the well-known p–y relations of Reese et al. (1974) and Matlock (1970) are used for sand and clay, respectively.

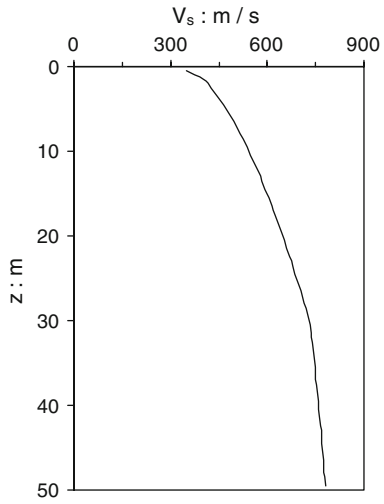

Fig. 4 Shear wave velocity distribution of the adopted soil deposit used for the wave propagation analysis

2.4 Soil profiles, seismic excitations, and site response analysis

The influence of soil amplification on the seismic response of the soil–pile-structure system is not examined, mainly for two reasons: (a) a thorough investigation of seismic ground response is out of scope of this paper, and (b) the unavoidable differences in free-field motions from the soil response analysis of the four different soil profiles, would complicate the comprehension of the related phenomena. Therefore, a single soil profile was selected for ground response analysis (Fig. 4): a category C profile, according to NEHRP (1994). Bedrock was assumed to be at 50 m depth.

The influence of shaking on the seismic response is investigated by selecting three real acceleration records as seismic excitations:

- the record from Aegion earthquake (1995),
- the record from Lefkada earthquake (2003), and
- the JMA record from Kobe earthquake (1995).

The first two records are representative strong motions of the seismic environment of Greece, with one and many cycles, respectively. JMA record is used to investigate the dynamic response of the soil–pile-structure system to a quite unfavorable incident. The dominant periods of the acceleration time histories for the aforementioned three earthquake records range from 0.2 to 0.8 s, resulting in a fixed base fundamental period ratio (designated as the fixed base fundamental period of the superstructure divided by the predominant period of the free-field surface acceleration time history) which ranges from 0.66 to 2.67. This is a wide range of values which ensures generalization of the results presented herein. Near-fault effects such as "rupture-directivity" and "fling" (Gerolymos et al. 2005) are also captured by the utilized accelerograms.

All the records were first scaled to a PGA of 0.5 g and 0.8 g at the ground surface; then through deconvolution analyses conducted with SHAKE (Schnabel et al. 1972), the bedrock motion as well as the motion at various depths along the pile, were estimated. The ground motion profiles obtained from SHAKE analyses are then used as input motion in the developed BNWF model. The acceleration time histories at the surface and the corresponding

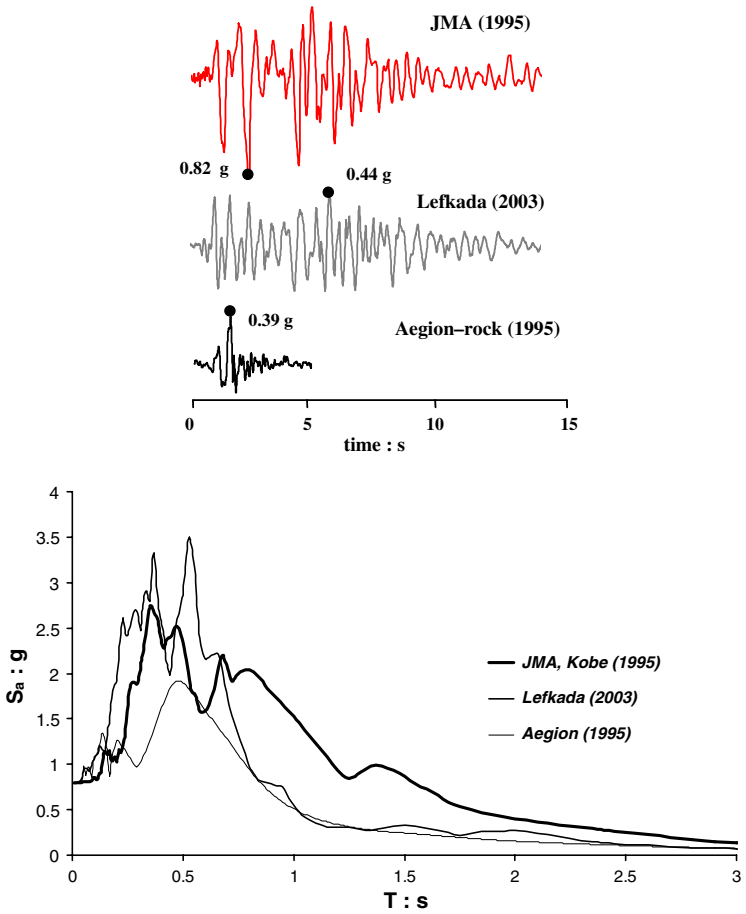

Fig. 5 Real acceleration time histories used as seismic excitation, after scaling to a peak ground acceleration of $a_g = 0.8\,\mathrm{g}$, and corresponding ($\xi = 5\%$) response spectra scaled to Sa (T = 0 s) = 0.8 g

elastic response spectra scaled to a SA (T = 0 s) = 0.8 g for 5% damping, are presented in Fig. 5.

It should be stated here in that from a seismological point of view, simply scaling an acceleration time history to a large PGA value for representing the severity of an earthquake might not be always correct. It is well known from the literature that high peak ground accelerations are usually accompanied by a large number of predominant cycles. Obviously, this is not the case for Aegion record which can be satisfactorily approximated by a single sinusoidal pulse.

2.5 Analysis methodology and performance measure parameters

Besides the fundamental response amounts (acceleration, displacement, moments, etc.) that describe the behavior of a structure under dynamic loading, other important seismic performance measures are the local and global ductility demand μ_φ and μ_δ, and the maximum drift ratio γ_{max}.

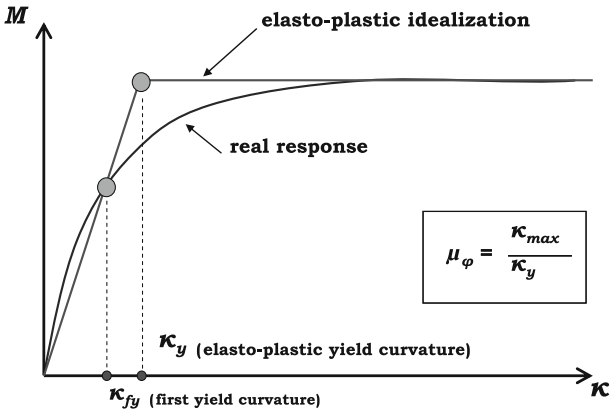

Fig. 6 Definition of yield curvature of the soil-pile-structure system

The local (curvature) ductility demand μ_φ is defined as the maximum curvature κ_{max} imposed on the structure by an earthquake, divided by the yield curvature κ_y, which is a property of the pile-column cross-section.

$$\mu_\varphi = \frac{\kappa_{\max}}{\kappa_y} \tag{8}$$

For bridge structures supported on extended piles, the local ductility demand imposed on the pile shaft might govern the design of the system, because damage to the pile (such as spalling of cover concrete, crack widths, potential for buckling or fracture of longitudinal reinforcement) is related to the local curvature ductility.

The following procedure is followed for the assessment of local curvature ductility demand in the analyses conducted. The moment–curvature curve of each pile-column cross-section is approximated by a bilinear elastic–perfectly plastic relation, in which the first (linear) section is defined as the secant stiffness through the first-yield point κ_{fy} (yielding of first longitudinal reinforcement bar) and the second section by the tangent line on the post-yielding section of the actual moment–curvature curve. The intersection of these two lines defines the cross-section yield curvature κ_y (Fig. 6).

Similarly, the global (displacement) ductility demand μ_δ is the ratio of the maximum displacement of the system u_{max}, imposed by an earthquake, to the yield displacement u_y, which is a soil–pile-structure system property.

$$\mu_\delta = \frac{u_{\max}}{u_y} \tag{9}$$

The yield displacement u_y is assessed through static nonlinear analyses (push-over analyses) according to the following procedure:

At the center of mass of the superstructure, a horizontal force is gradually applied. The maximum displacement and the curvature along the pile-column are continuously monitored. The *displacement measured, when the pile curvature reaches the first-yield point* κ_{fy}, is defined as the first-yield displacement u_{fy}. Then, similarly to the procedure followed for the determination of yield curvature, the load–displacement curve is approximated by an equivalent bilinear elastic–perfectly plastic curve, in which the first (linear) section is defined as the secant stiffness through the first-yield point u_{fy} and the second section by the tangent

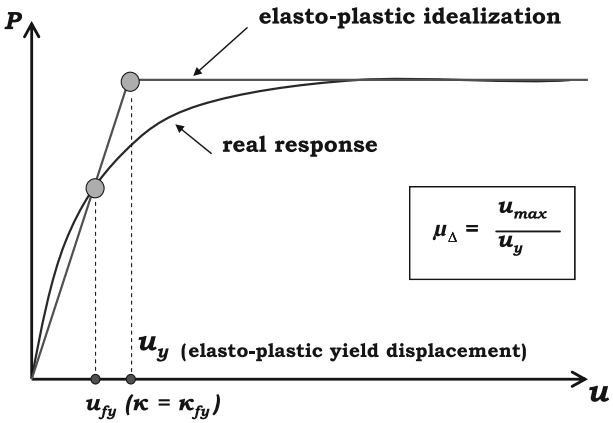

Fig. 7 Definition of yield displacement of the soil-pile-structure system

line on the post-yielding section of the load–displacement curve. The intersection of these two lines defines the yield displacement u_y (Fig. 7).

It has to be noticed, that for the estimation of pile curvature, we did not use the FEM original curvature results as these showed mesh sensitivity. Instead, plastic rotation results which are mesh insensitive, were used and divided by the plastic hinge length L_p to derive pile curvature. The length of plastic hinge L_p for the pile-columns was estimated according to Budek et al. (2000) approximation:

$$L_p = d + 0.06 \cdot H \tag{10}$$

where d is the pile diameter and H the above-ground height. Similar expressions, based however on different assumptions, have also been provided in Caltrans (1986, 1990), Dowrick (1987), Priestley et al. (1996), Chai (2002) and Chai and Hutchinson (2002).

The drift ratio γ is defined as the maximum displacement of the deck imposed by an earthquake relative to pier base displacement divided by the height of the pier:

$$\gamma = \frac{u_{\max}^{deck} - u_{\max}^{pier-base}}{H} \tag{11}$$

3 Analysis: results and discussion

In this paragraph, typical results of the nonlinear analyses are presented in terms of acceleration time-histories; peak bending moment, curvature and displacement distributions.

Results of the seismic response of the examined structural systems are presented in Figs. 8, 9, 10, 11, 12, 13, 14, 15, 16, 17, 18, 19, 20, 21, 22, 23, 24, 25, 26, 27, 28, 29, and 30. The acceleration time histories calculated for a pile-column of diameter $d = 3$ m and height $H = 5$ m are presented in Fig. 8 for every soil profile examined. The response of the deck is quite smaller in case of soft clay. On the contrary, stiff foundation soils lead to increased response of deck. An exception to this is the increased structural (deck) response for the case of loose sand. A possible explanation is that the lateral confinement providing by the soil might be considerable even for small values of internal friction angles of the soil, thus stiffening the response of the pile.

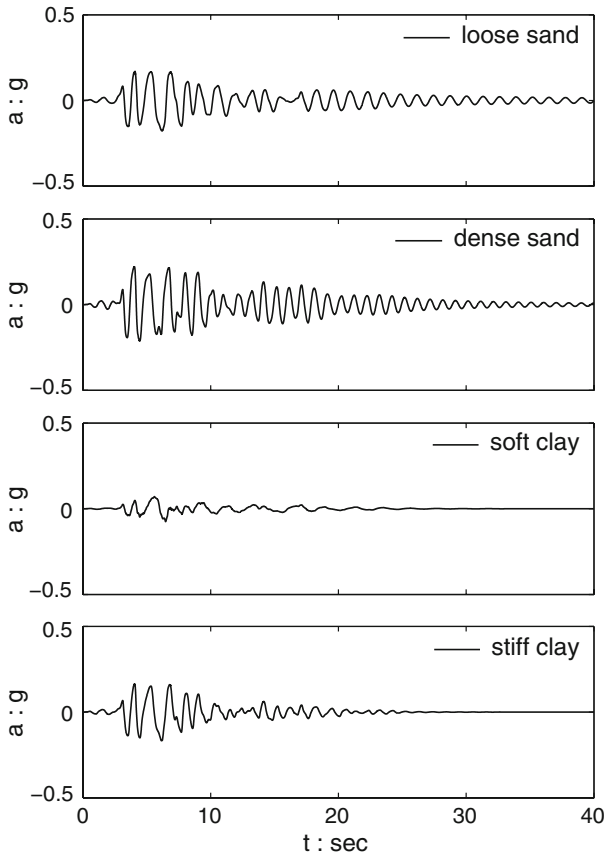

Fig. 8 Acceleration time histories of the deck for free-head pile-columns with aboveground height $H = 5$ m and diameters $b = d = 3.0$ m (excitation at ground surface: JMA, Kobe 1995—$a_g = 0.5$ g)

Similarly, differences are observed in Fig. 9, where the acceleration time histories of a 5 m high pier embedded in soft clay are illustrated for different pile diameters. Smaller pile-column diameter leads to higher deck acceleration. The small pile-column diameters ($d = 1.5$, 2.0 m) correspond to a deck mass which is 16 times smaller than that for the larger pile-column diameters ($d = 3.0, 4.0$ m). This substantial difference in deck masses is responsible for an also large discrepancy in the fundamental natural periods of the pier-foundation-soil system (effective periods). Indeed, as can be hardly seen in the response acceleration time histories after the input motion has subsided, at t = 15 s (free response), the effective period of the small-diameter bridge columns is approximately 1.0 s while that of the large-diameter bridge columns is about 2.0 s. It is therefore shown that the effective period of the pier systems increases with increasing mass of deck, despite that the fixed-base period is held constant. A similar trend in the response of bridge-piers supported either by a single pile or by a group of piles has been also shown in Gerolymos et al. (1998).

Furthermore, a small decrease in peak acceleration values is observed in constant-diameter extended pile ($d = 1.5$, 3.0 m) compared to the response of variable-diameter systems ($d = 2.0$, 4.0 m). The response of the constant-diameter systems is associated with more intense pile and soil inelasticity compared to the response of variable-diameter systems.

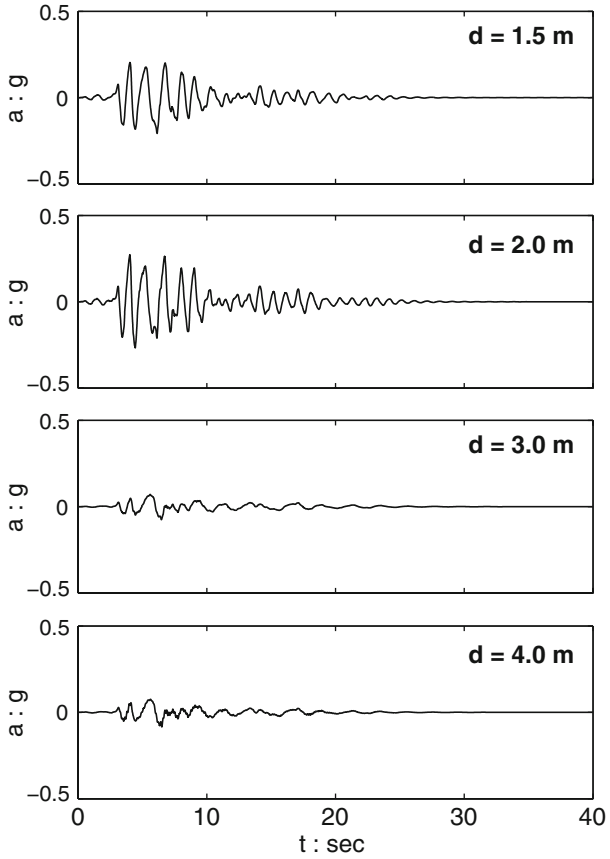

Fig. 9 Acceleration time histories of the deck for free-head pile-columns with aboveground height $H = 5$ m founded in soft clay (excitation at ground surface: JMA, Kobe 1995—$a_g = 0.5$ g)

The ample mobilization of soil plastification and structural yielding mechanisms in the case of constant-diameter piers results in an increase of both hysteretic and radiation damping, which in turn slows down the deck response.

The distributions of maximum displacements with depth for several cases are presented in Figs. 10 and 11 for the JMA record as seismic excitation at ground surface. The influence of soil in this distribution is depicted in Fig. 10: the softer the soil, the larger the maximum displacement within the soil. The increased compliance of the soft soils implies significant deflection of the pile. In Fig. 11, the role of pile diameter on the system response is illustrated. larger pile-diameter piers ($d = 3.0$ and 4.0 m) are associated with larger effective periods compared to those of smaller pile-diameter ($d = 1.5$ and 2.0 m). Given the response spectra of the JMA acceleration time history, this means that the larger pile-diameter systems exhibit larger displacements and smaller response accelerations compared to the piers with smaller pile diameters (see also Fig. 9).

The distributions of maximum bending moments with depth for several cases are presented in Figs. 12, 13, 14. The influence of soil type in this distribution is depicted in Fig. 12. Like in displacement distributions, soft soils result to increased pile effective lengths. With

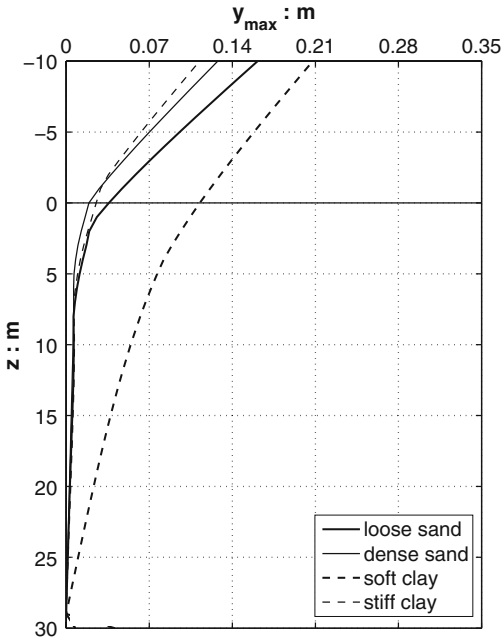

Fig. 10 Maximum displacement distributions for free-head pile-columns with aboveground height $H = 10$ m and diameters $b = d = 3.0$ m (excitation at ground surface: JMA, Kobe 1995—$a_g = 0.5$ g)

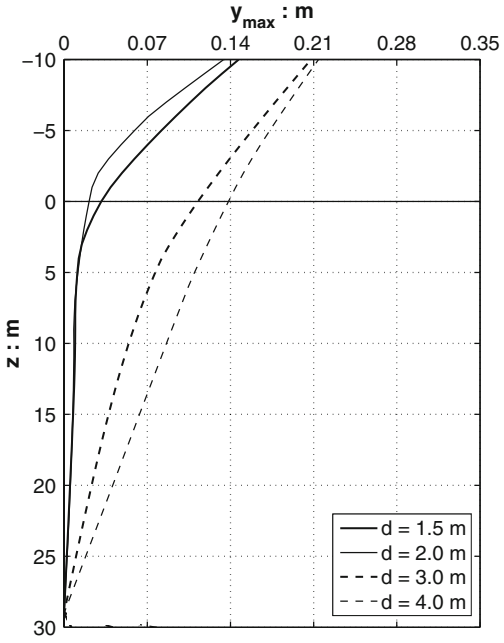

Fig. 11 Maximum displacement distributions for free-head pile-columns with aboveground height $H = 10$ m founded in soft clay (excitation at ground surface: JMA, Kobe 1995—$a_g = 0.5$ g)

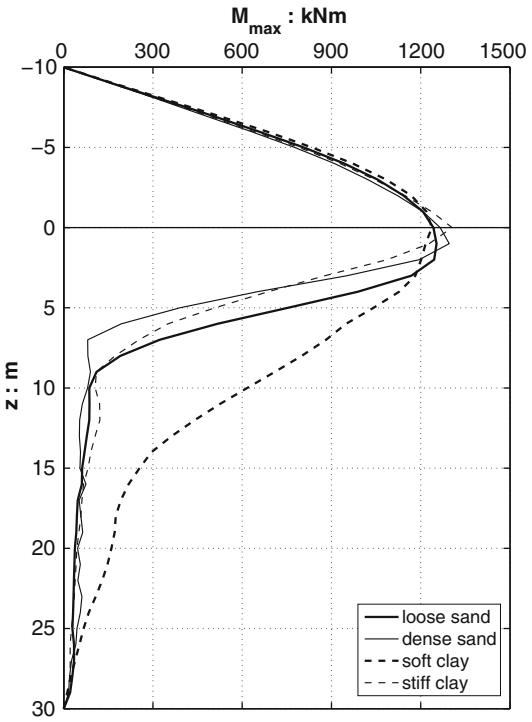

Fig. 12 Maximum bending moment distributions for free-head pile-columns with aboveground height $H =$ 10 m and diameters $b = d = 1.5$ m (excitation at ground surface: JMA, Kobe 1995—$a_g = 0.8$ g)

a maximum moment of 1200 kNm (yield moment), the depth where this value becomes half increases from 4 m, in case of stiff clay and dense sand, to 6 m for loose sand, and to 10 m in case of soft clay. It is interesting to observe in Fig. 12 that the maximum bending moments among the four cases are almost equal, indirectly revealing the formation of plastic hinges at certain locations of the piles. Given the severity of the gound motion (the JMA record scaled to a peak ground acceleration of 0.8 g), mobilization of the full bending moment resistance of the piles is unavoidable irrespectively of the type of foundation soil.

As shown in Figs. 13 and 14, the increase of pile diameter results to shifting of the maximum-moment depth to greater depths. It is noticed, that the maximum-moment depth does not always coincide with plastic hinge position, due to difference in pile and pier diameters.

The position of plastic hinge is easily assessed via distributions of pile curvature with depth. In Fig. 15, the distributions of curvature are presented for a 3-m diameter pile-column with above-ground height $H = 10$ m, embedded in different soils. It is observed that the plastic hinge is developed within 2 diameters below ground surface. The amplitude of curvature increases significantly in stiffer soils. The effect of pile diameter is shown in Fig. 16. In case of pile-columns with pier of smaller diameter than that of the pile ($d = 2.0$, 4.0 m), the pier is highly stressed and the plastic hinge is formed at its base. Below the ground surface, curvature values decrease rapidly. On the other hand, constant-diameter pile-columns ($d = 1.5$, 3.0 m) may develop plastic hinge below surface. In every case, however, plastic rotations are distributed in greater length with consequent decrease of the maximum curvature.

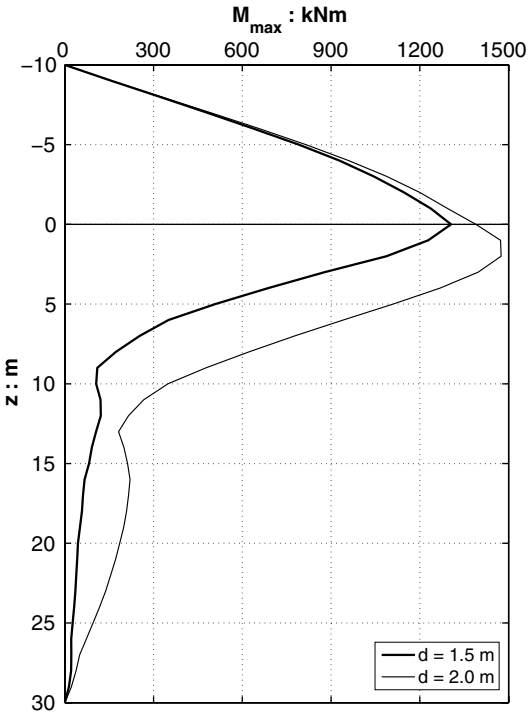

Fig. 13 Maximum bending moments distributions for free-head pile-columns with aboveground height $H =$ 10 m founded in stiff clay (excitation at ground surface: JMA, Kobe 1995—$a_g = 0.8$ g)

In Fig. 17, the correlation of the local curvature ductility demand to the global displacement ductility demand is presented. All the analyses resulted to nonlinear behavior of the extended pile shaft ($\mu_\delta > 1$) are depicted categorized according to the foundation soil. The mean ratio $(\mu_\varphi - 1)/(\mu_\delta - 1)$ equals to 5.4 for soft clay, 3.4 for loose sand, 2.6 for dense sand, and 2.7 for stiff clay. Similar results have been also obtained by Hutchinson et al. (2004). At first sight, it seems that founding pile-columns in soft soils is unfavorable: for a given earthquake imposed global displacement ductility, the local curvature ductility demand is higher than the one corresponds to stiffer soils. This impression, as will be revealed later on, may be deceptive.

A similar trend appears in Fig. 18 where analyses results have been categorized according to the potential location of plastic hinge. For constant-diameter pile-columns the plastic hinge is likely developed below the ground surface (on pile) whereas for variable-diameter pile-columns, plastic hinges are developed at the base of pier. The average ratio $(\mu_\varphi - 1)/(\mu_\delta - 1)$ takes a value of 3.5 for plastic hinge on the pile, and 2.7 for plastic hinge on the pier. The results discourage the inelastic design of pile, however, the picture is yet to be cleared.

In the next figures (Figs. 19 and 20), analyses results have been grouped according to pier diameter and shaking intensity, in respect. A slight predominance of the larger pier ($d = 3.0$ m) is observed as the average value of $(\mu_\varphi - 1)/(\mu_\delta - 1)$ ratio is 3.3 instead of 3.7 in case of smaller pier ($d = 1.5$ m). As expected, the shaking amplitude does not affect the value of ductility demand ratio.

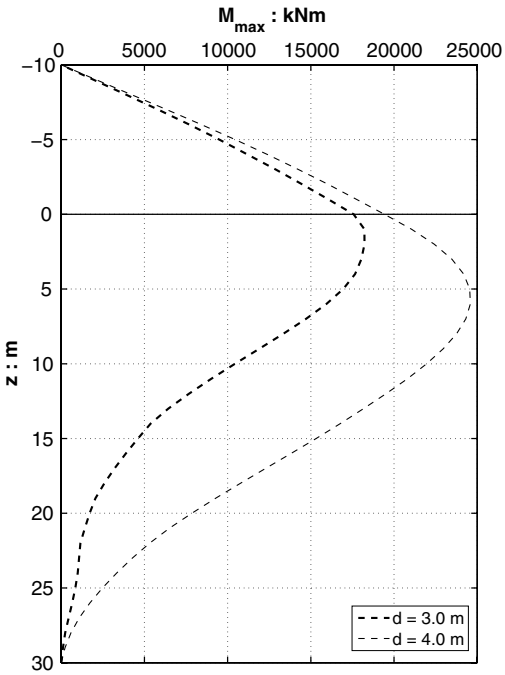

Fig. 14 Maximum bending moments distributions for free-head pile-columns with aboveground height $H = 10$ m founded in stiff clay (excitation at ground surface: JMA, Kobe 1995—$a_g = 0.8$ g)

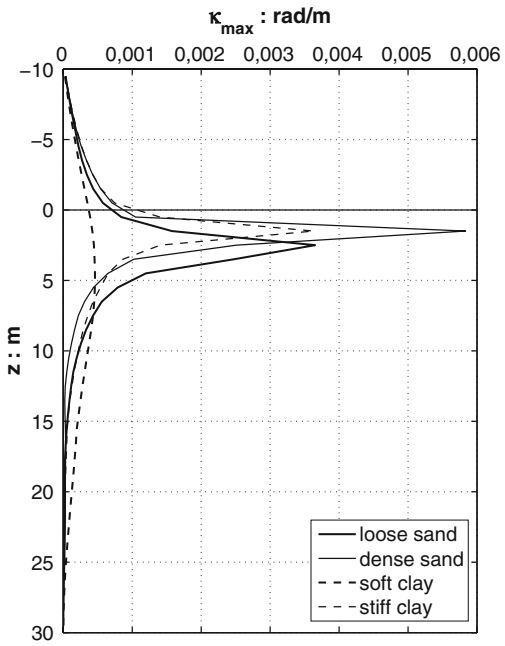

Fig. 15 Maximum curvature distributions for free-head pile-columns with above-ground height $H = 10$ m and diameter $d = 3.0$ m (excitation at ground surface: JMA, Kobe 1995—$a_g = 0.5$ g)

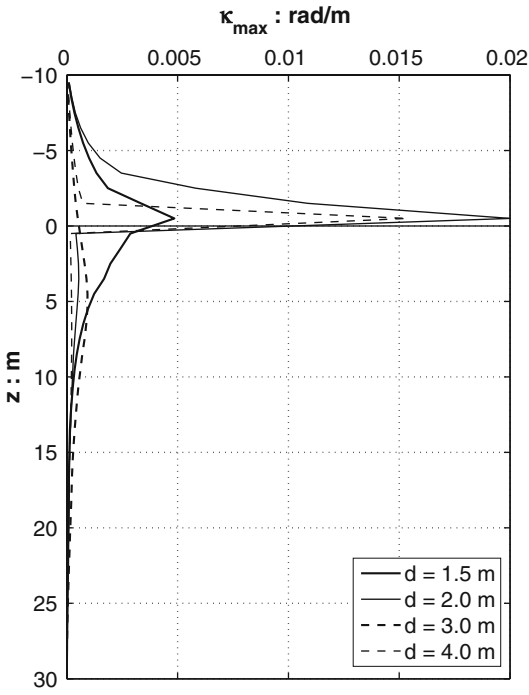

Fig. 16 Maximum curvature distributions for free-head pile-columns with above-ground height $H = 10$ m founded in soft clay (excitation at ground surface: JMA, Kobe 1995—$a_g = 0.8$g)

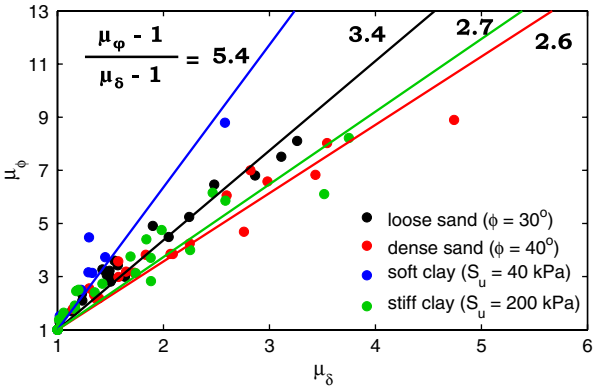

Fig. 17 Correlation of local and global ductility demands for different soil types

The influence of above-ground height H on the correlation between local and global ductility demand is illustrated in Fig. 21. Shorter piers exhibit greater local curvature ductility demand for a given displacement ductility level.

In Fig. 22, the correlation of local curvature ductility demand to the maximum drift ratio is presented for all the soil profiles examined. For a given maximum drift ratio, the required curvature ductility is greater for stiffer soils. The depth of the plastic hinge location increases

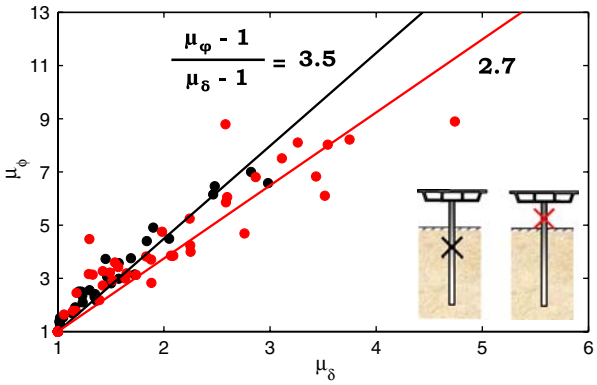

Fig. 18 Correlation of local and global ductility demands for different plastic hinge locations

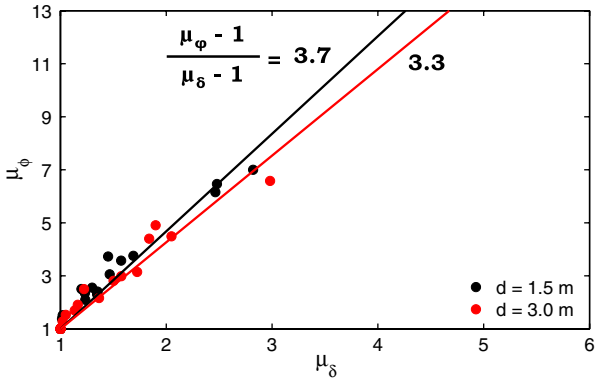

Fig. 19 Correlation of local and global ductility demands for different diameters

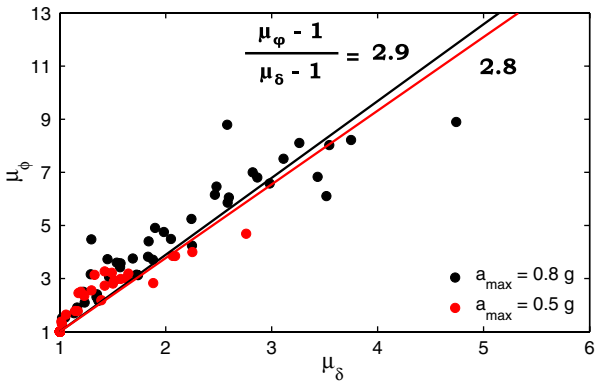

Fig. 20 Correlation of local and global ductility demands for different seismic motion amplitudes

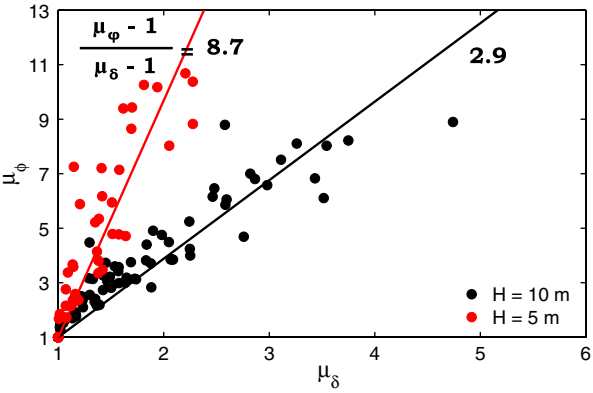

Fig. 21 Correlation of local and global ductility demands for different above-ground heights

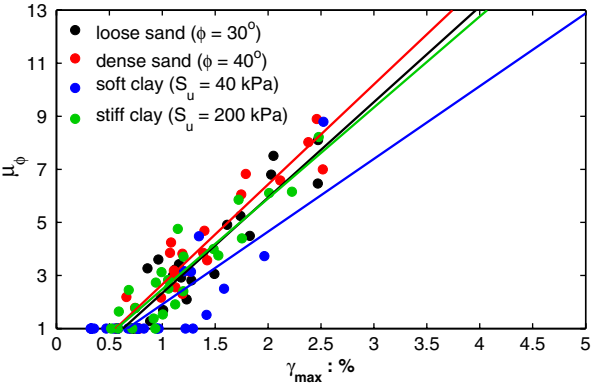

Fig. 22 Correlation of local ductility demand and maximum drift ratio for different soil types

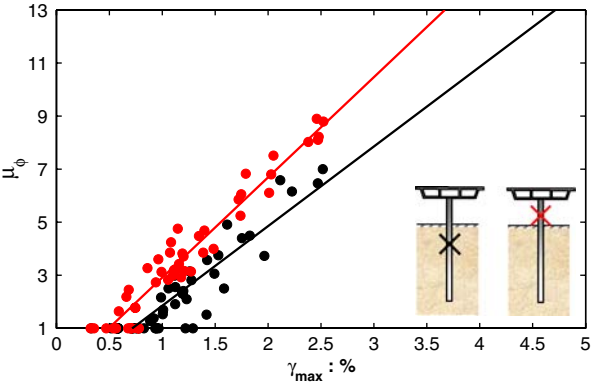

Fig. 23 Correlation of local ductility demand and maximum drift ratio for different plastic hinge locations

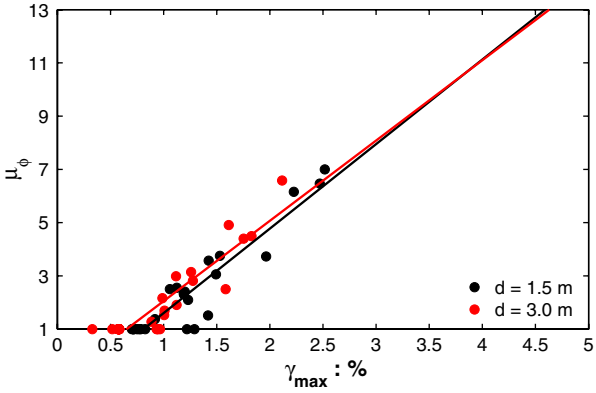

Fig. 24 Correlation of local ductility demand and maximum drift ratio for different diameters

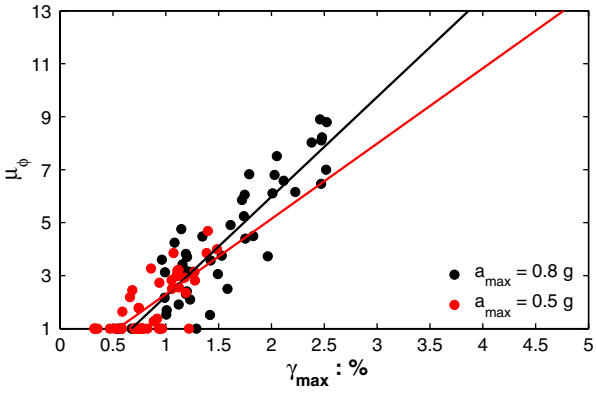

Fig. 25 Correlation of local ductility demand and maximum drift ratio for different seismic motion amplitudes

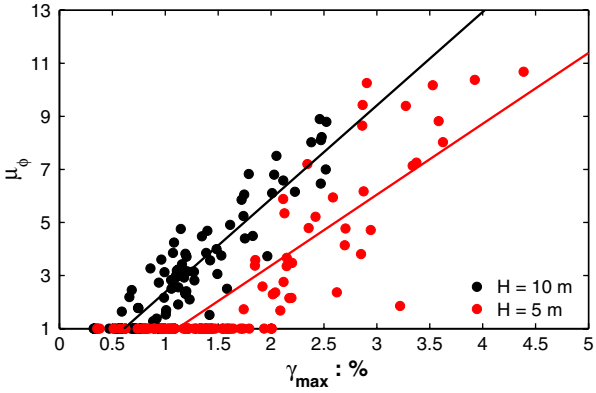

Fig. 26 Correlation of local ductility demand and maximum drift ratio for different above-ground heights

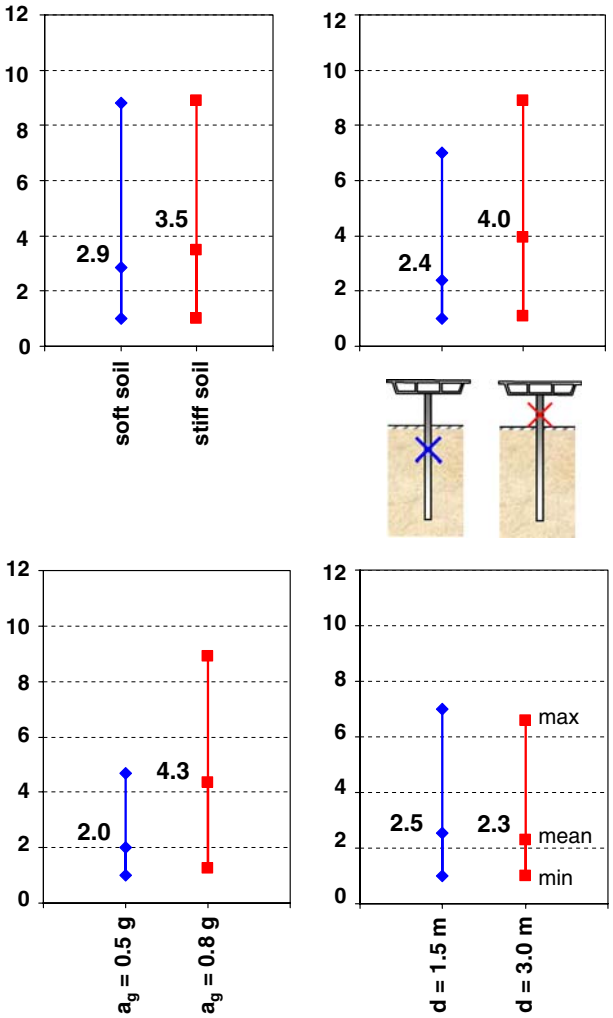

Fig. 27 Variation of local curvature ductility (μ_φ) demand for different parameters examined

with decreasing soil stiffness resulting in larger rigid body displacement, which however is not associated with strain in the pier. An inversion in the trend observed earlier is evident.

The same trend is observed in Fig. 23, where the effect of plastic hinge location is examined: for a given maximum drift ratio, the required curvature ductility is greater when the pier is plasticized. Indeed, the rigid body motion component of the displacement which increases with increasing depth of plastic hinge location, does not produce any structural damage and hence does not affect the ductility demand on the pier.

The pile-column diameter and the amplitude of ground motion only slightly affect the μ_φ/γ_{max} ratio (Figs. 24 and 25). The influence of above-ground height H on the correlation between local ductility demand and maximum drift ratio is illustrated in Fig. 26. Taller piers exhibit greater local curvature ductility demand for a given drift ratio. Indeed, for a given drift ratio the differential horizontal displacement between deck and pier base decreases with

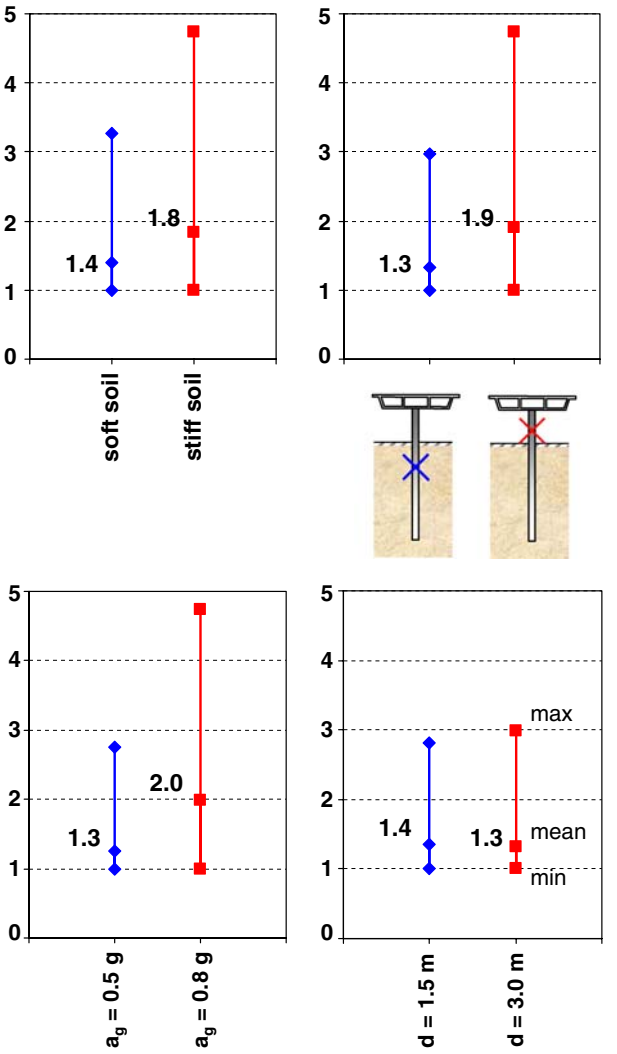

Fig. 28 Variation of global curvature ductility (μ_δ) demand for different parameters examined

decreasing above-ground height of the pier, leading to smaller pier distress and thus to smaller ductility demand.

In Figs. 27, 28, 29, and 30, the mean and peak values of the factors $\mu_\varphi \mu_\delta$, and γ_{max} are illustrated for various parameters examined. It is clearly observed that the mean and maximum values of both μ_φ and μ_δ factors are lower for soft soils and plasticized piles. This phenomenon discredits the trend appeared in Figs. 27 and 28 and reveals the beneficial influence of soil compliance and pile inelasticity on the response of the structure examined. The apparent paradox stems from the fact that kinematic expressions do not distinguish between capacity and demand, as also stated in Mylonakis et al. (2000). For example, according to Fig. 17, for a given displacement ductility demand the curvature ductility capacity of a pile-column embedded in soft soil needs to be larger than that of a pile-column embedded in

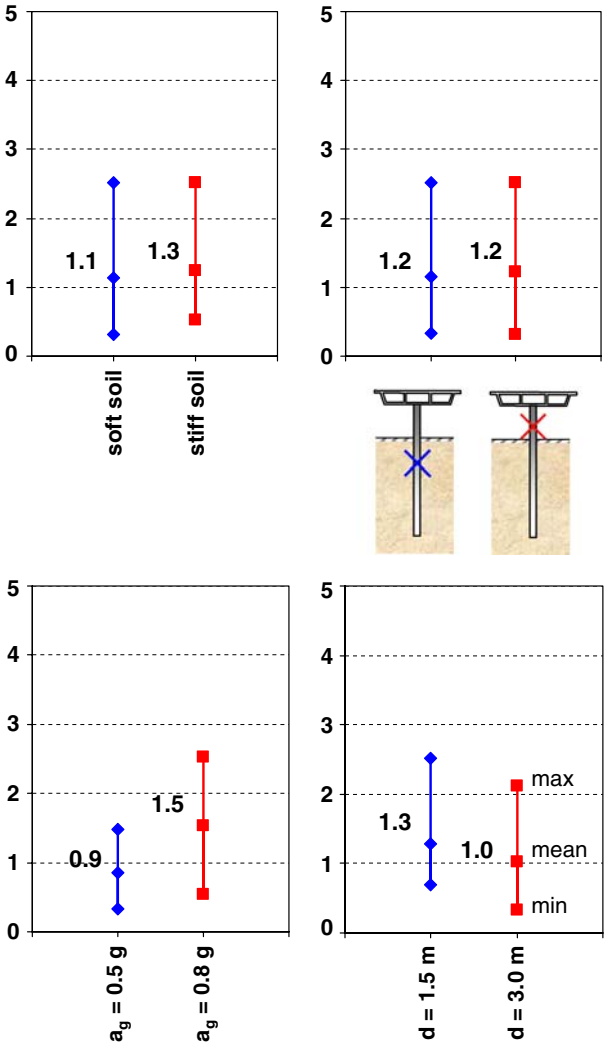

Fig. 29 Variation of maximum drift ratio (γ_{max}: %) for different parameters examined

stiff soil. However, this does not mean that for a given seismic excitation both pile-columns would exhibit the same displacement ductility.

Although the ratio $(\mu_\varphi - 1)/(\mu_\delta - 1)$ may take higher values for soft soils, the absolute values of μ_δ are small and so are the values of μ_φ. The maximum drift ratio γ_{max} seems to stay insensitive to parameters like soil stiffness and location of plastic hinges (Fig. 29). On the contrary, it depends strongly on the intensity of the seismic excitation. Increase of the above-ground height, as shown in Fig. 30, causes increase in the mean values of μ_δ and decrease in the mean value of γ_{max}, whereas mean μ_φ value slightly increases, if not remain constant.

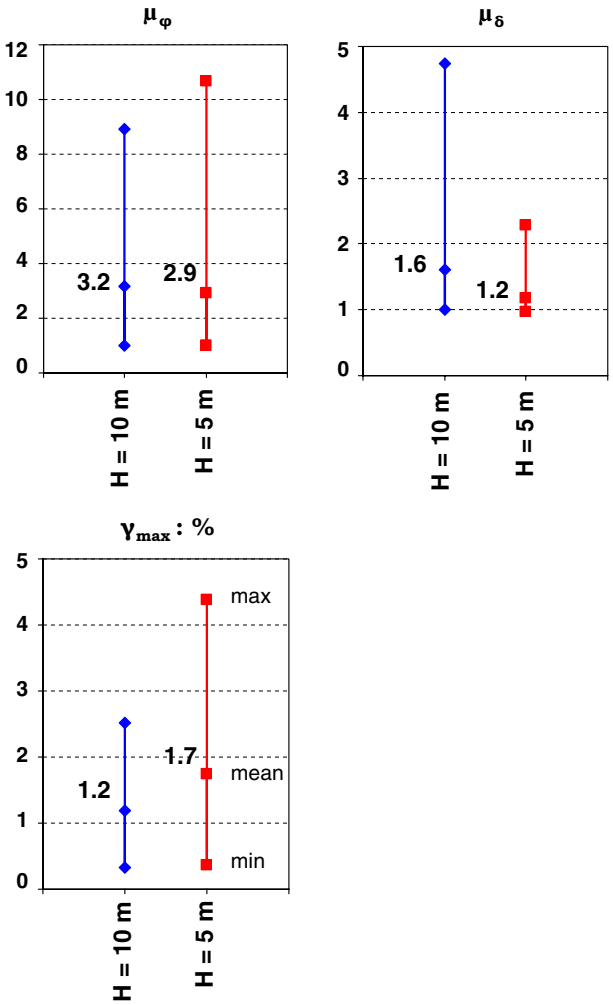

Fig. 30 Variation of performance measures for different above-ground heights

4 Conjectures

From the analysis of the results of the exploratory parametric analyses conducted herein, the following conclusions could be drawn:

For a given global (displacement) ductility demand $\mu_\delta(M–u)$,

- the local (curvature) ductility demand μ_φ increases for increased soil compliance.
- The potential formation of plastic hinge below ground surface also increases the local (curvature) ductility demand $\mu_\varphi(M–\kappa)$.
- The curvature ductility demand slightly decreases with increasing pile diameter.
- The curvature ductility demand increases in case of column-piles with Smaller above-ground height ratios (d/H).

The opposite trends for the local ductility demand μ_φ are observed, when the maximum drift ratio γ_{max} is kept constant.

However, the conclusions above do not reveal the true nature of the problem and the following remarks should be considered:

- For a given earthquake, the global displacement ductility demand μ_δ decreases as the soil compliance increases. Thus, while $(\mu_\varphi - 1)/(\mu_\delta - 1)$ ratio has a higher value for a soft soil, the small μ_δ demand may refrain the local ductility demand μ_φ at levels lower than what corresponds to a stiffer soil.
- The same comment holds for the location of plastic hinge. The potential of plastic hinge development on the pile (i.e. below ground surface) reduces μ_δ demand, with consequent reduction of local ductility demand.

Most of the available relations for the performance measures in literature are functions of structure geometry and reinforcement details only. However, from the results presented in this paper, the need for modification of these expressions in order to include soil-compliance and pile-plastification effects on structure dynamic response is demonstrated. Some very early, improved μ_φ–μ_δ correlations are proposed herein.

Nevertheless, it has to be noted that ductility capacity required in a structure does not always coincides with ductility demand which depends on the characteristics of the seismic loading and inelasticity of soil-pile-structure system. Thus, a structure with higher required ductility capacity may experience lower developed ductility than another structure with lower ductility capacity requirements. The actual ductility demands of a structure can be assessed "accurately" exclusively within the framework of a nonlinear dynamic analysis, in which the influence of soil properties and excitation characteristics are parametrically investigated.

Acknowledgments The research reported herein was sponsored by the General Secretariat for research (ΓΓΕΤ), in the course of ASPROGE project.

References

ATC-32—Applied Technology Council (1996) Improved seismic design criteria for California bridges: provisional recommendations. ATC-32, Redwood City, California

Banerjee S, Stanton JF, Hawkins NM (1987) Seismic performance of precast concrete bridge piles. J Struct Eng 113(2):381–396

Broms B (1964a) Lateral resistance of piles in cohesive soils. J Soil Mech Found Div, ASCE 90(3):27–63

Broms B (1964b) Lateral resistance of piles in cohesionless soils. J Soil Mech Found Div, ASCE 90(3): 123–156

Budek AM, Priestley MJN, Benzoni G (2000) Inelastic seismic response of bridge drilled-shaft RC pile/columns. J Geotech Geoenviron Eng 126(4):510–517

Caltrans (1986) Bridge design specifications manual. Caltrans, Sacramento, California

Caltrans (1990) Bridge design specifications/seismic design references. Caltrans, Sacramento, California

Chai YH (2002) Flexural strength and ductility of extended pile-shafts. I: analytical model. J Struct Eng 128(5):586–594

Chai YH, Hutchinson TC (2002) Flexural strength and ductility of extended pile-shafts. II: experimental study. J Geotech Geoenviron Eng 128(5):595–602

Chapman HE (1995) Earthquake resistant bridges and associated highway structures: current New Zealand practice. Proc., National Seismic Conference on Bridges and Highways, San Diego, California

Dowrick DJ (1987) Earthquake resistant design. 2nd edition. Wiley-Interscience, New York

Gazetas G, Dobry R (1984) Simple radiation damping model for piles and footings. J Eng Mech, ASCE 110:937–956

Gerolymos N, Gazetas G (2005a) Constitutive model for 1-D cyclic soil behavior applied to seismic analysis of layered deposits. Soils Found 45(3):147–159

Gerolymos N, Gazetas G (2005b) Phenomenological model applied to inelastic response of soil–pile interaction systems. Soils Found 45(4):119–132
Gerolymos N, Gazetas G (2006a) Development of Winkler model for static and dynamic response of Caisson foundations with soil and interface nonlinearities. Soil Dyn Earthq Eng 26(5):363–376
Gerolymos N, Gazetas G (2006b) Static and dynamic response of massive Caisson foundations with soil and interface nonlinearities—validation and results. Soil Dyn Earthq Eng 26(5):377–394
Gerolymos N, Gazetas G, Mylonakis G (1998) Fundamental period and effective damping of pile-supported bridge piers. Eleventh European conference on earthquake engineering, Paris (in CD Rom)
Gerolymos N, Apostolou M, Gazetas G (2005) Neural network analysis of the overturning response under near-fault type excitation. Earthq Eng Eng Vib 4(2):213–228
Hutchinson TC, Boulanger RW, Chai YH, Idriss IM (2004) Inelastic seismic response of extended pile shaft supported bridge structures. Report PEER 2002/14, Pacific Earthquake Engineering Research Center, University of California, Berkeley
Makris N, Gazetas G (1992) Dynamic pile-soil-pile interaction. Part II: Lateral and seismic response. Earthq Eng Struct Dyn 21:145–162
Matlock H (1970) Correlations for design of laterally loaded piles in soft clay. Proc., 2nd annual offshore technology conference, Houston, Texas, pp 577–594
Mazzoni S, McKenna F, Fenves GL (2005) OpenSees command language manual. The Regents of the University of California, Berkeley, p 375
Mylonakis G, Gazetas G, Gerolymos N, Anastasopoulos I (2000) Detrimental role of soil-structure interaction and the collapse of the 18-Pier Fukae bridge in Kobe. In: Katsikadelis JT, Beskos DE, Gdoutos E (eds) Recent advances in applied mechanics, honorary volume for Professor A.N.Kounadis. N.T.U.A., Athens, pp 145–159
NEHRP (1994) Recommended provisions for seismic regulations of new buildings: part 1, provisions. FEMA 222A, National Earthquake Hazard Reduction Program, Federal Emergency Management Agency, Washington, DC
Park R (1998) New Zealand practice on the design of bridges for earthquake resistance. Proc., 1st structural engineers world congress. Elsevier Science, San Francisco
Priestley MJN, Seible F, Calvi GM (1996) Seismic design and retrofit of bridges. Wiley-Interscience, New York
Reese LC, Cox WR, Koop FD (1974) Analysis of laterally loaded piles in sand. Proc., 6th annual offshore technology conference, Houston, Texas, pp 473–485
Schnabel PB, Lysmer J, Seed HB (1972) SHAKE—a computer program for earthquake response analysis of horizontally layered sites. EERC 72-12, Univ. of Calif., Berkeley